Hindawi
International Journal of Photoenergy
Volume 2017, Article ID 1625274, 11 pages
https://doi.org/10.1155/2017/1625274

Research Article

Effect of Fe Loading Condition and Reductants on CO_2 Reduction Performance with Fe/TiO_2 Photocatalyst

Akira Nishimura,[1] Noriaki Ishida,[1] Daichi Tatematsu,[1] Masafumi Hirota,[1] Akira Koshio,[2] Fumio Kokai,[2] and Eric Hu[3]

[1]*Division of Mechanical Engineering, Graduate School of Engineering, Mie University, 1577 Kurimamachiya-cho, Tsu, Mie 514-8507, Japan*
[2]*Division of Chemistry for Materials, Graduate School of Engineering, Mie University, Tsu, Mie 514-8507, Japan*
[3]*School of Mechanical Engineering, The University of Adelaide, North Terrace, Adelaide, SA 5005, Australia*

Correspondence should be addressed to Akira Nishimura; nisimura@mach.mie-u.ac.jp

Received 23 March 2017; Revised 19 June 2017; Accepted 10 July 2017; Published 9 August 2017

Academic Editor: Elisa Isabel Garcia-Lopez

Fe-doped TiO_2 (Fe/TiO_2) film photocatalyst was prepared by sol-gel and dip-coating process and pulse arc plasma method. The effect of pulse number on the CO_2 reduction performance with the Fe/TiO_2 was investigated in this study. In addition, the effect of reductants such as H_2O, H_2, and NH_3/H_2O on the CO_2 reduction performance with the Fe/TiO_2 photocatalyst was also investigated. The characteristics of the prepared Fe/TiO_2 film coated on a netlike glass fiber which is a base material were analyzed by SEM, EPMA, EDX, and EPMA. Furthermore, the CO_2 reduction performance of the Fe/TiO_2 film was tested under a Xe lamp with or without ultraviolet (UV) light. The results show that the CO_2 reduction performance with the pulse number of 100 is the best with H_2O and/or H_2 as reductant under UV light illumination, while that with the pulse number of 500 is the best when NH_3/H_2O is used as reductant. On the other hand, the CO_2 reduction performance with the pulse number of 500 is the best under every reductant condition without UV light illumination. The highest CO_2 reduction performance with the Fe/TiO_2 is obtained under $H_2 + H_2O/CO_2$ condition, and the best moral ratio of total reductants to CO_2 is 1.5 : 1.

1. Introduction

Due to mass consumption of fossil fuels, global warming and fossil fuel depletion have become serious global environmental problems in the world. After the industrial revolution, the averaged concentration of CO_2 in the world has been increased from 278 ppmV to 400 ppmV by 2015 [1]. Therefore, it is necessary to develop a new CO_2 reduction or utilization technology in order to recycle CO_2.

There are six vital CO_2 conversions: chemical conversions, electrochemical reductions, biological conversions, reforming, inorganic conversions, and photochemical reductions [2, 3]. Recently, artificial photosynthesis or the photochemical reduction of CO_2 to fuel has become an attractive route due to its economically and environmentally friendly behavior [2].

TiO_2 is the principle catalyst for almost all types of photocatalysis reaction. It is well known that CO_2 can be reduced into fuels, for example, CO, CH_4, CH_3OH, and H_2 by using TiO_2 as the photocatalyst under ultraviolet (UV) light illumination [4–9]. If this technique could be applied practically, a carbon circulation system would then be established: CO_2 from the combustion of fuel is reformed to fuels again using solar energy, and true zero emission can be achieved. However, the CO_2 reduction rate using pure TiO_2 is very low, that is, the fuel concentration in the products is very low. In addition, pure TiO_2 is only photoactive at a wavelength below 400 nm due to its relatively large bandgap energy (~3.2 eV) [10].

Recently, studies on CO_2 photochemical reduction by TiO_2 have been carried out from the viewpoint of performance promotion by extending absorption range towards visible region [11–15]. Noble metal doping such as Pt, Pd, Au, and Ag [11], nanocomposite CdS/TiO_2 combining two different band gap photocatalysts [12], N_2-modified TiO_2 [13], light harvesting complex of green plants assisted Rh-doped TiO_2 [14], and dye-sensitized TiO_2 [15] have been attempted to overcome the shortcomings of pure TiO_2. They did improve the CO_2 reduction performance; however, the concentrations in the products achieved in all the attempts so far were still low, ranging from 10 ppmV to 1000 ppmV [4–6, 9] or from 1 μmol/g-cat to 100 μmol/g-cat [7, 8, 11–15]. Therefore, a big breakthrough in increasing the concentration level of products is necessary to advance the CO_2 reduction technology in order to make the technology practically useful.

It was reported that doping transition metal was a useful technique for extending the absorbance of TiO_2 into the visible region [16]. For doping, various metal ions have been used, but among them, Fe^{3+} is considered as a strong candidate as it has a similar radius to Ti^{4+} (Fe^{3+} = 78.5 pm, Ti^{4+} = 74.5 pm) [17] and can easily fit into the crystal lattice of TiO_2 [16, 18, 19]. Moreover, the redox potential (energy differential) of Fe^{2+}/Fe^{3+} is close to that of Ti^{3+}/Ti^{4+}, resulting in shifting its optical absorption into the visible region [16, 18, 19]. Due to easy availability as well as the above described characteristics, Fe is selected as the dopant in the present study.

In the present paper, TiO_2 film is coated by sol-gel and dip-coating process on net glass fiber (SILIGLASS U, Nihonmuki Co.). Netlike glass fiber is a net composed of glass fiber whose diameter is about 10 μm. The fine glass fibers are knitted, resulting in a diameter of the aggregate fiber of about 1 mm. According to manufacturer specifications of the netlike glass fiber, the porous diameter of glass fiber is about 1 nm and the specific surface area is about 400 m^2/g. The netlike glass fiber consists of SiO_2 whose purity is over 96 wt%. The aperture of the net is about 2 mm × 2 mm. Since the netlike glass fiber has a porous characteristic, it is believed that the TiO_2 film is captured by the netlike glass fiber easily during a sol-gel and dip-coating process. In addition, it can be expected that CO_2 absorption performance of prepared photocatalyst is promoted due to the porous structure of the netlike glass fiber.

Then, Fe is loaded on the TiO_2-coated netlike glass fiber by pulse arc plasma method which can emit nanosized Fe particles by applying high electrical potential difference. Since the amount of loaded Fe can be controlled by pulse number, the present paper investigates the impact of the pulse number on characterization and CO_2 reduction performance of the prepared Fe/TiO_2.

To promote the CO_2 reduction performance of photocatalyst, it is important to select the optimum reductant which provides the proton for the reduction reaction. Generally speaking, H_2O is used as a reductant for CO_2 reduction by photocatalyst according to some review papers [20–23]. The reaction scheme of CO_2 reduction with H_2O is as follows [4, 24–26].

Photocatalytic reaction:

$$TiO_2 + h\nu \rightarrow h^+ + e^- \quad (1)$$

Oxidization:

$$\begin{aligned} H_2O + h^+ &\rightarrow \cdot OH + H^+ \\ \cdot OH + H_2O + h^+ &\rightarrow O_2 + 3H^+ \end{aligned} \quad (2)$$

Reduction:

$$CO_2 + 2H^+ + 2e^- \rightarrow CO + H_2O \quad (3)$$

H_2 is also a good candidate for the reductant since H_2 can be converted into a proton by photocatalyst [27–36]. The reaction scheme of CO_2 reduction with H_2 is as follows [30].

Photocatalytic reaction:

$$TiO_2 + h\nu \rightarrow h^+ + e^- \quad (4)$$

Oxidization:

$$H_2 + 2h^+ \rightarrow 2H^+ + 2e^- \quad (5)$$

Reduction:

$$\begin{aligned} CO_2 + e^- &\rightarrow \cdot CO_2^- \\ \cdot CO_2^- + 2H^+ + 2e^- &\rightarrow CO + CO_3^{2-} \\ \cdot CO_2^- + H^+ + e^- &\rightarrow HCOO^- \\ HCOO^- + H^+ &\rightarrow CO + H_2O \end{aligned} \quad (6)$$

Though there are some reports on CO_2 reduction with H_2 [27–36], there are few reports investigating the reaction with TiO_2 as the photocatalyst is a few [27–31]. Particularly, there is no study on CO_2 reduction with Fe/TiO_2. This paper investigates the reduction performance of Fe/TiO_2 for CO_2 with H_2 as well as CO_2 with H_2O. Furthermore, the present paper also investigates the effect of $NH_3 + H_2O$ on CO_2 reduction performance with the Fe/TiO_2 as the photocatalyst since NH_3 is thought to be a good H_2 carrier. According to the authors' review, there is no report on CO_2 reduction over Fe/TiO_2 with NH_3. NH_3 is thought to be used as reductant directly since NH_3 aqueous solution can decompose into H_2 and N_2 by photocatalyst [37]. After decomposition of NH_3, it is believed that the reaction scheme of CO_2 reduction with H_2 can be applied.

In this paper, TiO_2 film doped with Fe (Fe/TiO_2) was prepared and characterized by scanning electron microscope (SEM), electron probe microanalyzer (EPMA), transmission electron microscope (TEM), and energy dispersive X-ray spectrometry (EDX) analysis to clarify the optimum amount of loaded Fe. The CO_2 reduction characteristics of Fe/TiO_2 coated on net glass fiber with H_2O and/or H_2 and NH_3 under the condition of illuminating Xe lamp with or without UV light were investigated.

2. Experiment

2.1. Preparation of Fe/TiO$_2$ Film. Sol-gel and dip-coating process was used for preparing TiO_2 film. TiO_2 sol solution was made by mixing $[(CH_3)_2CHO]_4Ti$ (purity of 95 wt%, Nacalai Tesque Co.) of 0.3 mol, anhydrous C_2H_5OH (purity of 99.5 wt%, Nacalai Tesque Co.) of 2.4 mol, distilled water of 0.3 mol, and HCl (purity of 35 wt%, Nacalai Tesque Co.) of 0.07 mol. The netlike glass fiber was cut to disc, and its diameter and thickness were 50 mm and 1 mm, respectively. The netlike glass fiber was dipped into TiO_2 sol solution at the speed of 1.5 mm/s and pulled up at a fixed speed of 0.22 mm/s. Then, it was dried out and fired under the controlled firing temperature (FT) and firing duration time (FD), resulting in the TiO_2 film fastened on the base material. FT and FD were set at 623 K and 180 s, respectively. Fe was loaded on the TiO_2 film by pulse arc plasma method. The pulse arc plasma gun device (ULVAC Inc., ARL-300) having an Fe electrode whose diameter was 10 mm was applied for Fe loading. After the netlike glass fiber coated with TiO_2 was set in the chamber of the pulse arc plasma gun device, which was vacuumed, the nanosized Fe particles were emitted from the Fe electrode applying an electrical potential difference of 200 V. The pulse arc plasma gun can evaporate an Fe particle over the target in the circle area whose diameter is 100 mm when the distance between the Fe electrode and the target is 160 mm. Since the difference between Fe electrode and TiO_2 film was 150 mm in the present study, Fe particle can be evaporated over the TiO_2 film uniformly. The amount of loaded Fe was controlled by pulse number. In the present paper, the pulse number was set at 100, 500, and 1000.

2.2. Characterization of Fe/TiO$_2$ Film. The structure and crystallization characteristics of Fe/TiO_2 film were evaluated by SEM (JXA-8530F, JEOL Ltd.), EPMA (JXA-8530F, JEOL Ltd.), TEM (JEM-2100F/HK, JEOL Ltd.), and EDX (JEM-2100F/HK, JEOL Ltd.). Since these measuring instruments use electron for analysis, the sample should be an electron conductor. Since the netlike glass disc is not an electron conductor, the carbon vapor deposition was conducted by the dedicated device (JEE-420, JEOL Ltd.) for Fe/TiO_2 coated on a netlike glass disc before analysis. The thickness of carbon deposited on samples was approximately 20–30 nm.

The electron probe emits the electrons to the sample under the acceleration voltage of 15 kV and the current of 3.0×10^{-8} A, when the surface structure of sample is analyzed by SEM. The characteristic X-ray is detected by EPMA at the same time, resulting in the concentration of chemical element analyzed according to the relationship between the characteristic X-ray energy and the atomic number. The spatial resolution of SEM and EPMA is 10 μm. The EPMA analysis helps not only to understand the coating state of prepared photocatalyst but also to measure the amount of doped metal within TiO_2 film on the base material.

The electron probe emits the electron to the sample under the acceleration voltage of 200 kV, when the inner structure of the sample is analyzed by TEM. The size, thickness, and structure of loaded Fe were evaluated. The characteristic X-ray is detected by EDX at the same time,

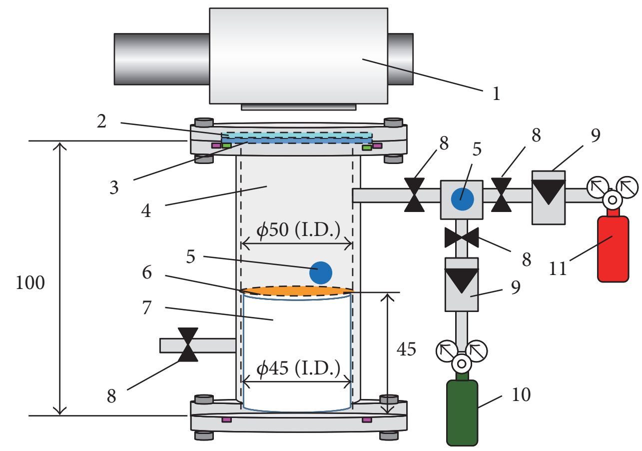

(1) Xelamp
(2) Sharp cut filter
(3) Quartz glass disc
(4) Stainless pipe
(5) Gas sampling tap
(6) Photocatalyst
(7) Teflon cylinder
(8) Valve
(9) Mass flow controller
(10) CO_2 gas cylinder (99.995 vol%)
(11) H_2 gas cylinder (99.99999 vol%)

Figure 1: Schematic drawing of CO_2 reduction experimental setup.

resulting in the concentration distribution of chemical element toward thickness direction of the sample being analyzed. In the present paper, the concentration distribution of Ti and Fe were analyzed.

2.3. CO$_2$ Reduction Experiment. Figure 1 shows the experimental setup of the reactor consisting of a stainless pipe (100 mm (*H.*) × 50 mm (*I.D.*)), a netlike glass disc coated with Fe/TiO_2 film which is located on the Teflon cylinder (50 mm (*H.*) × 50 mm (*D.*)), a quartz glass disc (84 mm (*D.*) × 10 mm (*t.*)), a sharp cut filter which cuts off the light of wavelength below 400 nm (SCF-49.5C-42L, SIGMA KOKI CO. LTD.), a 150 W Xe lamp (L2175, Hamamatsu Photonics K. K.), a mass flow controller, a CO_2 gas cylinder, and a H_2 gas cylinder.

The reactor volume available for CO_2 charge is 1.25×10^{-4} m^3. The light of the Xe lamp, through the sharp cut filter and the quartz glass disc that are at the top of the stainless pipe, illuminates the netlike glass disc coated with Fe/TiO_2 film, which is located inside the stainless pipe. The wavelengths of light from the Xe lamp are ranged from 185 nm to 2000 nm. The Xe lamp can be fitted with a sharp cut filter to remove UV components of the light. With the filter, the wavelengths of light from the Xe lamp are ranged from 401 nm to 2000 nm [38]. The average light intensity of the Xe lamp on the photocatalyst without and with setting the sharp cut filter is 57.5 mW/cm^2 and 43.7 mW/cm^2, respectively.

In the CO_2 reduction experiment with H_2O or NH_3 + H_2O, after purging the reactor chamber with CO_2 gas of the purity of 99.995 vol% flowed through the reactor for 15 minutes, the valves located at the inlet and the outlet of reactor were closed. After confirming the gas pressure and gas temperature in the reactor at 0.1 MPa and 298 K, respectively, the distilled water of 100 μL or NH_3 aqueous solution (NH_3: 50 vol%) of 200 μL was injected into the reactor through gas sampling tap, and the Xe lamp illumination was turned on

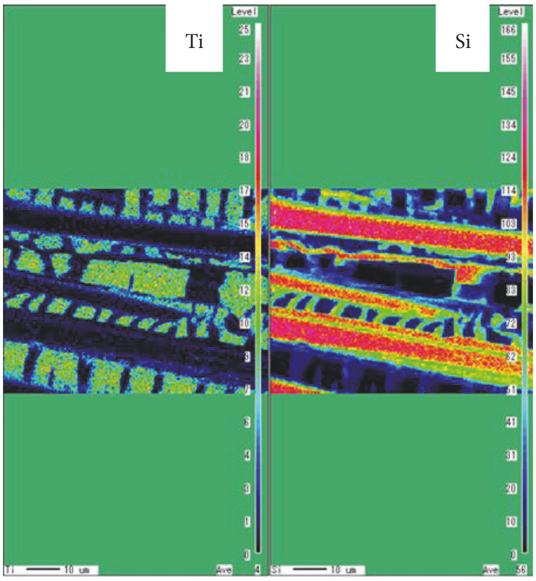

Figure 2: EPMA image of TiO_2 film.

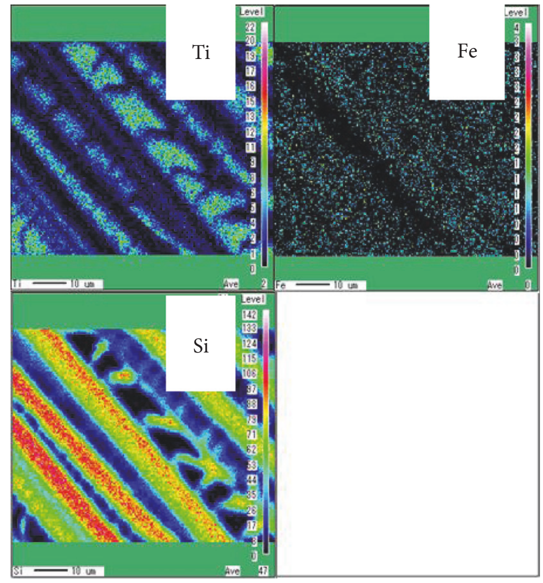

Figure 3: EPMA image of Fe/TiO_2(100) film.

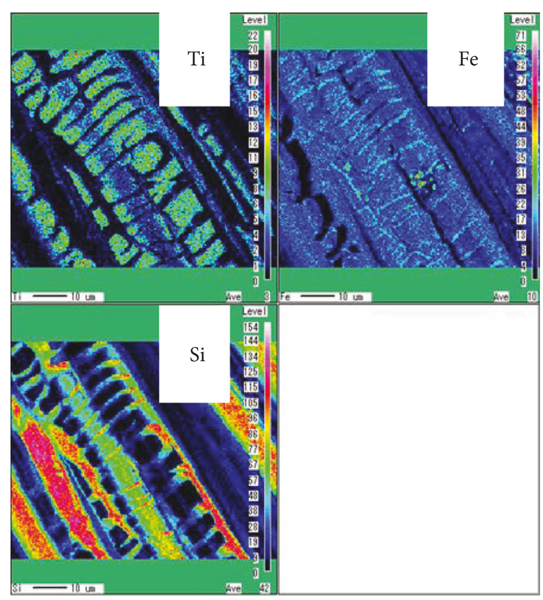

Figure 4: EPMA image of Fe/TiO_2(500) film.

at the same time. The water and NH_3 aqueous injected vaporized completely in the reactor. Due to the heat of the Xe lamp, the temperature in the reactor was attained at 343 K within an hour and kept at approximately 343 K during the experiment.

In the CO_2 reduction experiment with H_2, CO_2 gas with the purity of 99.995 vol% and H_2 gas with the purity of 99.99999 vol% which were controlled by mass flow controller were mixed in the buffer chamber and introduced in the reactor which was prevacuumed by a vacuum pump. After that, Xe lamp illumination was turned on. The mixing ratio of CO_2 and H_2 was confirmed by TCD gas chromatograph (Micro GC CP4900, GL Science) before introducing into the reactor. In the CO_2 reduction experiment with $H_2 + H_2O$, the distilled water was injected into the reactor after charging CO_2 and H_2.

In the CO_2 reduction experiment with H_2O or H_2, the molar ratio of H_2O or H_2 to CO_2 was 1 : 1. In the CO_2 reduction experiment with $NH_3 + H_2O$, the molar ratio of NH_3 and H_2O to CO_2 was 0.7 : 1 : 1. In the CO_2 reduction experiment with $H_2 + H_2O$, the molar ratio of H_2 and H_2O to CO_2 was set at 0.5 : 0.5 : 1, 1 : 1 : 1, 2 : 2 : 1, 1 : 0.5 : 1 and 1 : 1 : 0.5.

The gas in the reactor was sampled every 24 hours during the experiment. The gas samples were analyzed by FID gas chromatograph (GC353B, GL Science) and methanizer (MT221, GD Science). Minimum resolution of FID gas chromatograph and methanizer is 1 ppmV.

3. Results and Discussion

3.1. Characterization of Fe/TiO_2 Film. Figures 2–5 show EPMA images of TiO_2, Fe/TiO_2(100), Fe/TiO_2(500), and Fe/TiO_2(1000) film, respectively, where Fe/TiO_2(100) means TiO_2 with Fe loaded by the pulse number of 100. EPMA analysis was carried out for 1500 times magnification SEM images. In EPMA image, the concentrations of each element in observation area are indicated by the different colors. Light colors, for example, white, pink, and red, indicate that the amount of element is large, while dark colors like black and blue indicate that the amount of element is small.

From these figures, it can be observed that the TiO_2 film with teeth-like shape was coated on a netlike glass fiber. It is also seen that TiO_2 film builds a bridge among several glass fibers like reported also in [38]. During firing process, the temperature profile of TiO_2 solution adhered on the

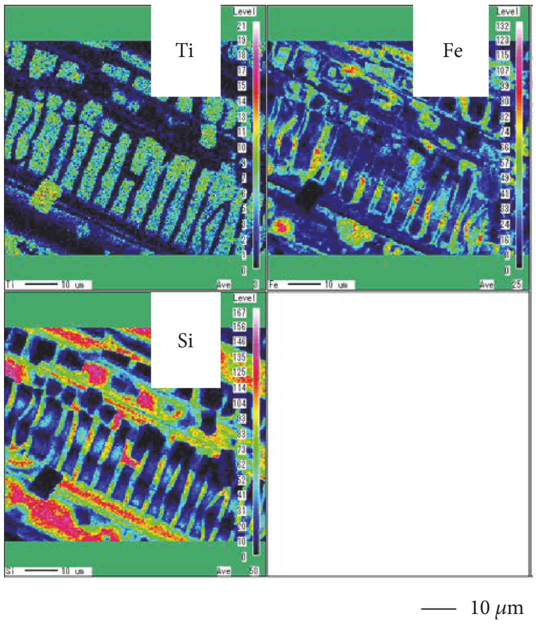

Figure 5: EPMA image of Fe/TiO_2(1000) film.

Table 1: Weight ratio of elements Fe and Ti within prepared Fe/TiO_2 film.

Photocatalyst type	Ti (wt%)	Weight ratio Fe (wt%)	Total (wt%)
Fe/TiO_2(100)	98.16	1.84	100.00
Fe/TiO_2(500)	79.27	20.73	100.00
Fe/TiO_2(1000)	46.47	53.35	100.00

netlike glass disc was not even due to the different thermal conductivities of Ti and SiO_2. The thermal conductivities of Ti and SiO_2 at 600 K are 19.4 W/(m·K) and 1.82 W/(m·K), respectively [39]. Due to the thermal expansion and shrinkage around the netlike glass fiber, a thermal crack formed on the TiO_2 film. Therefore, the TiO_2 film on the netlike glass fiber was teeth like.

It is observed from Figure 3 that nanosized Fe particles loaded on TiO_2 uniformly. On the other hand, it is revealed that the amount of loaded Fe increases with increasing the pulse number from Figures 4 and 5. In other words, there is an Fe layer covering TiO_2 for Fe/TiO_2(500) and Fe/TiO_2(1000).

To evaluate the amount of loaded Fe within the TiO_2 film quantitatively, the observation area, which is the center of netlike glass disc, of diameter of 300 μm, is analyzed by EPMA. The ratio of Fe to Ti in this observation area is counted by averaging the data obtained in this area. Table 1 gives the weight percentages of elements Fe and Ti in the Fe/TiO_2 film. From this table, it can be seen that more Fe is contained in the Fe/TiO_2 film with increasing pulse number. From these results, it is proved that the amount of dopants on a photocatalyst can be controlled by pulse arc plasm method quantitatively.

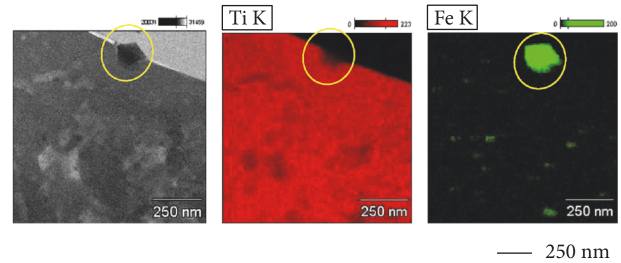

Figure 6: EDX image of Fe/TiO_2(100) film.

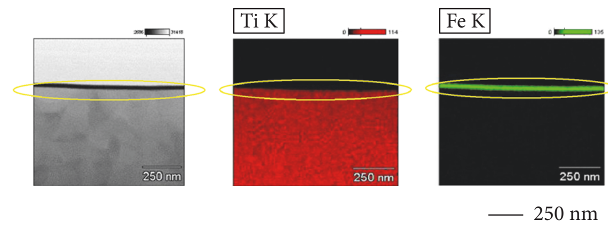

Figure 7: EDX image of Fe/TiO_2(500) film.

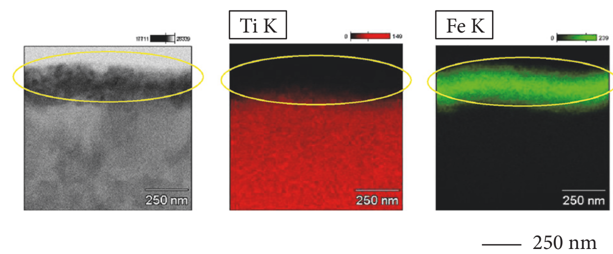

Figure 8: EDX image of Fe/TiO_2(1000) film.

Figures 6–8 show EDX images of Fe/TiO_2(100), Fe/TiO_2(500), and Fe/TiO_2(1000) film, respectively. EDX analysis was carried out using 150,000 times magnification TEM images. In these figures, the yellow circle indicates the existence of Fe.

According to Figure 6, it is observed that Fe particle is loaded on TiO_2 film. The average size of Fe particle for Fe/TiO_2(100) in the present study is approximately 28 nm where the longest length of Fe particle was used as a representative length. As to Fe/TiO_2(500) shown in Figure 7, there was an Fe layer covering the TiO_2 film. The average thickness of Fe layer for Fe/TiO_2(500) in the present study was found to be approximately 36 nm. For Fe/TiO_2(1000), the thickness of Fe layer was thicker than that on the Fe/TiO_2(500). The average thickness of Fe layer for Fe/TiO_2(1000) in the present study is approximately 230 nm. Since the pulse arc plasm was repeated continuously with such a large pulse number of 1000, the tip of Fe electrode was melted and a lump of Fe was emitted. Therefore, the thickness of Fe layer for Fe/TiO_2(1000) was remarkably longer than that for Fe/TiO_2(500).

3.2. Effect of Amount of Fe on CO_2 Reduction Performance of Fe/TiO_2. Figures 9–11 show the comparison of molar quantity of CO per weight of photocatalyst along the time under

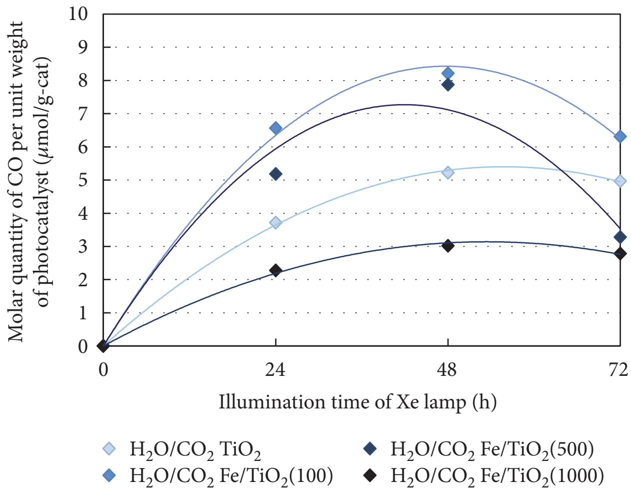

Figure 9: Comparison of CO_2 reduction performance of TiO_2 and Fe/TiO_2 with H_2O under illumination conditions with UV light.

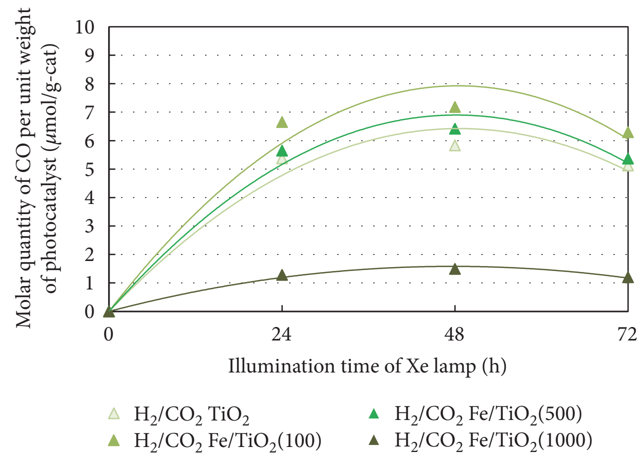

Figure 10: Comparison of CO_2 reduction performance of TiO_2 and Fe/TiO_2 with H_2 under illumination conditions with UV light.

the Xe lamp with the UV light on, for TiO_2 or Fe/TiO_2 film under H_2O/CO_2, H_2/CO_2, and $NH_3 + H_2O/CO_2$ condition, respectively. In this experiment, CO is the only fuel produced from the reactions. Since the concentrations of CO in most experiments started to decrease after illumination of 48–72 hours for illumination conditions with UV light due to the reverse reaction by CO and O_2, that is, the by-product, Figures 9–11 only show the concentration up to 72 hours. Before the experiments, a blank test, that was running the same experiment without illumination of Xe lamp, had been carried out to set up a reference case. No fuel was produced in the blank test as expected.

According to Figures 9 and 10, the molar quantity of CO per weight of photocatalyst for $Fe/TiO_2(100)$ is the highest among the prepared photocatalysts under H_2O/CO_2 and H_2/CO_2 conditions. Although the amount of Fe increases with increasing pulse number as shown in Table 1, Fe layer covers TiO_2 film according to EPMA and EDX analysis. When the metal covers TiO_2 surface, the light absorption ability is impaired and the contact between TiO_2 and CO_2 + reductant is blocked [40]. Consequently, the $Fe/TiO_2(100)$ which has enough area absorbing light and contacting reactants has the best CO_2 reduction performance. On the other hand, the molar quantity of CO per weight of photocatalyst for $Fe/TiO_2(500)$ is the highest among the prepared photocatalysts under $NH_3 + H_2O/CO_2$ condition. Since six electrons are necessary to decompose NH_3 into H_2 and N_2 by photocatalyst [37] and CO_2 reduction with H_2 also need two electrons after NH_3 decomposition as described in Section 1, more electrons are used under $NH_3 + H_2O/CO_2$ condition compared to H_2O/CO_2 and H_2/CO_2 conditions. Therefore, the $Fe/TiO_2(500)$ which can provide more electrons is the best photocatalyst even though Fe layer covers TiO_2 film. However, the CO_2 reduction performance of Fe/TiO_2 under $NH_3 + H_2O/CO_2$ condition is lower compared to that under H_2O/CO_2 and H_2/CO_2 conditions due to complicity of the reactions. In addition, a very thick Fe layer covers TiO_2 film for the $Fe/TiO_2(1000)$, resulting in a very low CO_2 reduction performance. The improvement of photocatalytic performance by Fe doping under the illumination condition with UV light is thought to be caused by the generation of shallow charge traps in the crystal structure which decreases the recombination rate of electron-hole pairs [18] except for $Fe/TiO_2(1000)$.

Figures 12–14 show the comparison of molar quantity of CO per weight of photocatalyst along the time under the Xe lamp illumination without UV light, for TiO_2 or Fe/TiO_2 film under H_2O/CO_2, H_2/CO_2, and $NH_3 + H_2O/CO_2$ condition, respectively. In this experiment, CO is the only fuel produced from the reactions. Since the concentration of CO almost started to decrease after illumination of 72–96 hours for most cases due to the reverse reaction by CO and O_2 which is by-product, Figures 12–14 only show the concentration up to 96 hours.

From Figures 12–14, it can be seen that the CO_2 reduction performance of TiO_2 is promoted by Fe doping due to extension of the photoresponsivity of TiO_2 [41] to the visible spectrum as well as decrease in the recombination rate of electron-hole pairs by the generation of shallow charge traps in the crystal structure. According to Figures 12–14, the molar quantity of CO per weight of photocatalyst for $Fe/TiO_2(500)$ is the highest among the prepared photocatalysts, which indicates that the larger pulse number is suitable for the illumination condition without UV light. Under the illumination condition without UV light, the amount of doped Fe is important to absorb the visible light in order to perform the photocatalytic reaction [41]. As to the $Fe/TiO_2(1000)$, since the too-high loading Fe covered the TiO_2 surface, the light absorption ability was impaired and the contact between TiO_2 and CO_2 + reductant was blocked [40], resulting in lower CO_2 reduction performance compared to the other pulse numbers.

3.3. Optimization of Reductant on CO_2 Reduction Performance of Fe/TiO_2. To investigate the combination effect of reductant, Figure 15 shows the comparison of molar quantity of CO per weight of photocatalyst along the time under the Xe lamp with UV light on, for $Fe/TiO_2(100)$ film under $H_2 + H_2O/CO_2$ condition. Due to the UV light

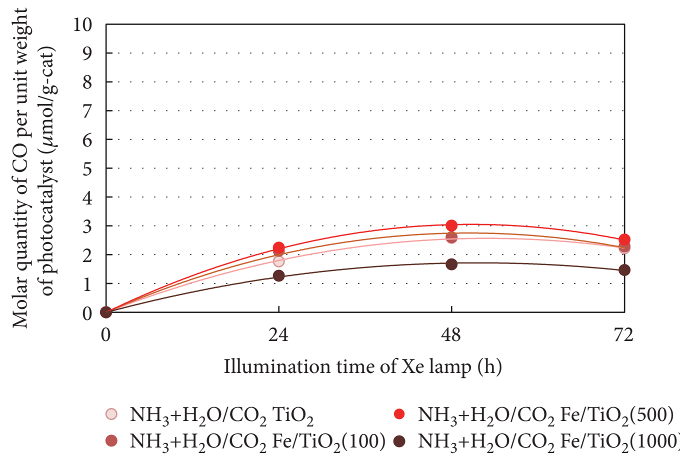

Figure 11: Comparison of CO_2 reduction performance of TiO_2 and Fe/TiO_2 with $NH_3 + H_2O$ under illumination conditions with UV light.

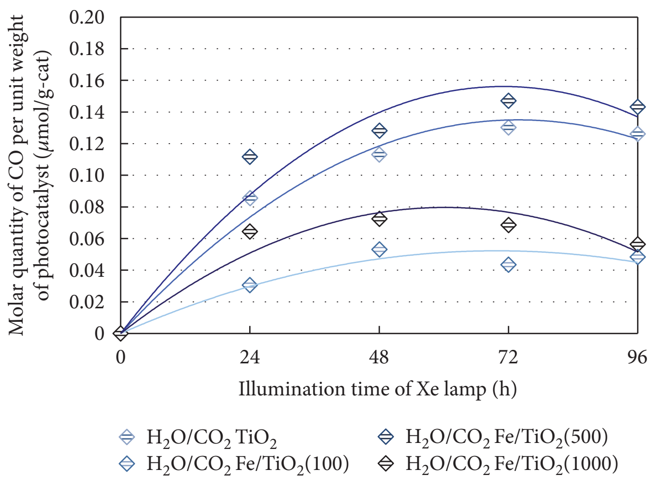

Figure 12: Comparison of CO_2 reduction performance of TiO_2 and Fe/TiO_2 with H_2O under illumination conditions without UV light.

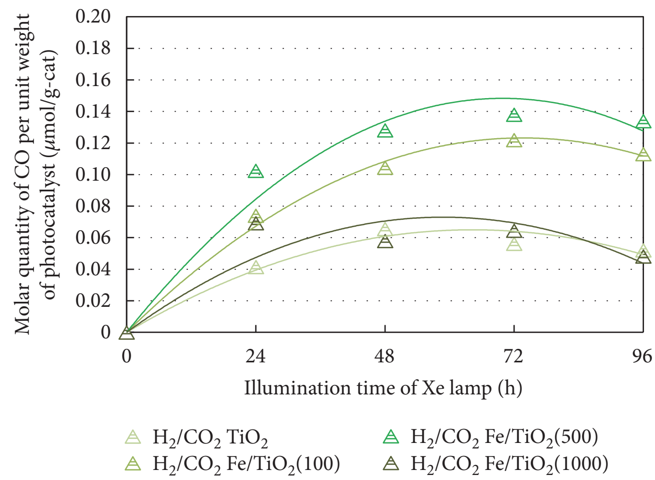

Figure 13: Comparison of CO_2 reduction performance of TiO_2 and Fe/TiO_2 with H_2 under illumination conditions without UV light.

illumination condition, $Fe/TiO_2(100)$ is selected as the best photocatalyst as described in Section 3.2. For comparison, the results under H_2O/CO_2 and H_2/CO_2 conditions are also shown in this figure. Since the present study wants to know the CO_2 reduction performance obtaining a larger amount of product, the results under the illumination condition with UV light are shown.

From Figure 15, it reveals that the molar quantity of CO per weight for Fe/TiO_2 under $H_2 + H_2O/CO_2$ condition is larger than the sum of that under H_2O/CO_2 and H_2/CO_2 conditions, which agrees with the report carried out by TiO_2 [30]. Simultaneous presence of H_2O and H_2 in the system have not changed the reaction pathway, but have accelerated the photoreduction of CO_2 with H_2, since H_2O donated electron to inhibit the recombination of electron and hole [30]. In addition, the molar ratio of H_2 and H_2O to CO_2 of 1 : 0.5 : 1 gives the best CO_2 reduction performance. However, the molar ratio of H_2 and H_2O to CO_2 of 0.5 : 1 : 1 shows the second best performance, which means the moral ratio of total reductants to CO_2 of 1.5 : 1 is optimal. According to reaction scheme of H_2O/CO_2 and H_2/CO_2 shown in Section 1, the theoretical molar ratio of CO_2 to H_2O or H_2 is 1 : 1. It is therefore believed that the excess amount of reductant is necessary for CO_2 reduction in practice.

Table 2 lists the maximum molar quantity of CO per weight of photocatalyst for each condition to summarize the CO_2 reduction performance of prepared photocatalysts in this study. According to Table 2, the molar ratio of H_2 and H_2O to CO_2 of 1 : 0.5 : 1 gives the best CO_2 reduction performance in this study as described above. Table 3 lists the initial rate of CO production for each condition to investigate the CO_2 reduction rate of prepared photocatalysts in this study. The initial rate of CO production is estimated by dividing the molar quantity of CO per weight of photocatalyst at 24 h by illumination time of 24 h. According to Table 3, the initial rate of CO production under $H_2 + H_2O/CO_2$ condition is larger than that under the other conditions. This indicates that the combination of H_2 and H_2O leads the

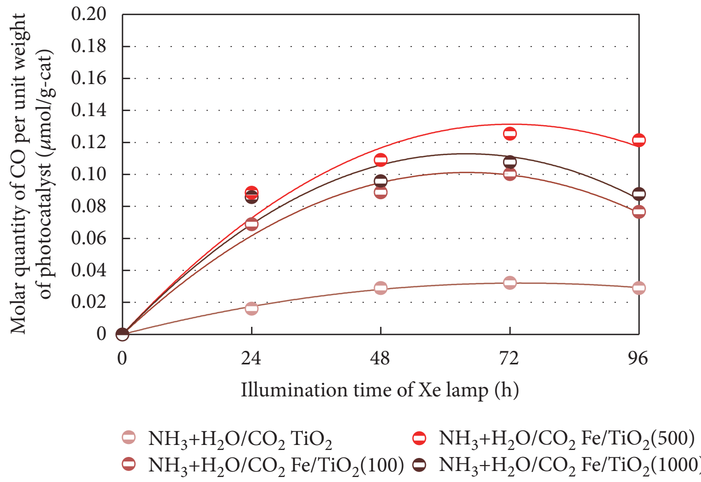

FIGURE 14: Comparison of CO_2 reduction performance of TiO_2 and Fe/TiO_2 with $NH_3 + H_2O$ under illumination conditions without UV light.

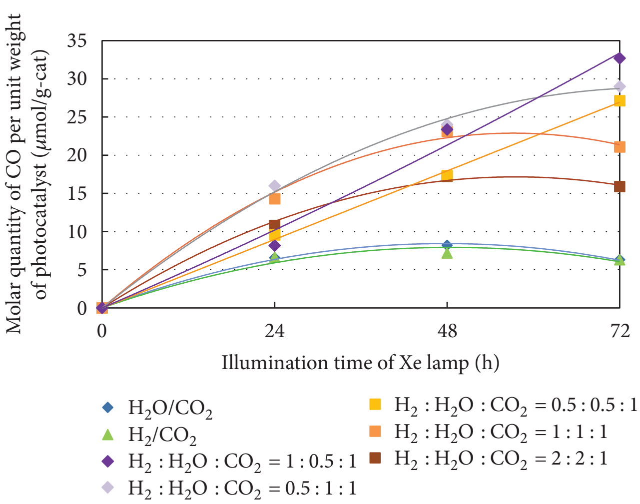

FIGURE 15: Impact of reductant combination on CO_2 reduction performance of $Fe/TiO_2(100)$ under illumination conditions with UV light.

fast reaction of prepared photocatalyst since H_2 and H_2O promote the reduction and oxidation reaction during photocatalysis reaction, respectively.

Compared to the previous research on CO_2 reduction with $H_2 + H_2O$ over pure TiO_2, the CO_2 reduction performance of photocatalysts prepared in this study is almost 100 times as large as that reported in [30], which is owing to Fe doping. Though reference [30] reported the CO production performance of ZrO_2 under $H_2 + H_2O/CO_2$ condition, the CO production performance of Fe/TiO_2 prepared by this study is approximately 30 times as large as that of ZrO_2. In addition, the other research [42] also reported the CO_2 reduction performance of TiO_2 under $H_2 + H_2O/CO_2$ condition. The CO production performance of Fe/TiO_2 prepared by this study is approximately 100 times as large as that reported in reference [42]. Since Fe doping provides the free electron preventing recombination of electron and hole produced as well as improving the light absorption effect, the big improvement of CO_2 reduction performance is obtained in the present study, which reaches almost the same level compared to the other studies [7, 8, 11–15], in terms of CO_2 reduction performance. One way to further promote the CO_2 reduction performance is double overlapping arrangement of Fe/TiO_2 coated on netlike glass disc. The authors have already reported that the double overlapping arrangement of Fe/TiO_2 coated on netlike glass disc was effective to improve CO_2 reduction performance of Fe/TiO_2 under H_2O/CO_2 condition since the electron transfer between two overlapped photocatalysts was promoted by overlapping [38]. In addition, the other dopants like Cu, which can absorb the longer wavelength light than Fe [19], should be used at lower positioned layers since the wavelength of penetrating light becomes long through higher positioned photocatalyst by losing energy [38]. This idea is similar to the concept of the hybrid photocatalyst using two photocatalysts having different band gaps [43–45].

In the rear future, this study would like to carry out the reusability evaluation on the structure characterization and photocatalytic activity, which are important to investigate the possibility of applying a photocatalyst in a practical way.

4. Conclusions

Based on the investigation in this study, the following conclusions can be drawn.

(1) TiO_2 could be coated on netlike glass fiber where it appears in teeth-like shape. Fe fine particles could be loaded onto the TiO_2 using the pulse arc plasma method with various pulse numbers. When the pulse number was over 500, there would be a Fe layer formed on the TiO_2.

(2) With the UV illumination condition, the molar quantity of CO per weight of photocatalyst for

Table 2: Comparison of CO_2 reduction performance of prepared photocatalysts in this study.

	TiO_2 (μmol/g)	Fe/TiO_2(100) (μmol/g)	Fe/TiO_2(500) (μmol/g)	Fe/TiO_2(1000) (μmol/g)
With UV				
H_2O/CO_2	5.2	8.2	7.9	3.0
H_2/CO_2	5.8	7.2	6.4	1.5
$NH_3 + H_2O/CO_2$	2.6	2.6	3.0	1.7
$H_2 : H_2O : CO_2 = 1 : 0.5 : 1$	N/A	33	N/A	N/A
$H_2 : H_2O : CO_2 = 0.5 : 1 : 1$	N/A	29	N/A	N/A
$H_2 : H_2O : CO_2 = 0.5 : 0.5 : 1$	N/A	27	N/A	N/A
$H_2 : H_2O : CO_2 = 1 : 1 : 1$	N/A	23	N/A	N/A
$H_2 : H_2O : CO_2 = 2 : 2 : 1$	N/A	17	N/A	N/A
Without UV				
H_2O/CO_2	5.3×10^{-2}	1.3×10^{-1}	1.5×10^{-1}	7.2×10^{-2}
H_2/CO_2	6.6×10^{-2}	1.2×10^{-1}	1.4×10^{-1}	6.9×10^{-2}
$NH_3 + H_2O/CO_2$	3.2×10^{-2}	1.0×10^{-1}	1.3×10^{-1}	1.1×10^{-1}

Table 3: Comparison of initial rate of CO production of prepared photocatalysts in this study.

	TiO_2 (μmol/(g·h))	Fe/TiO_2(100) (μmol/(g·h))	Fe/TiO_2(500) (μmol/(g·h))	Fe/TiO_2(1000) (μmol/(g·h))
With UV				
H_2O/CO_2	1.6×10^{-1}	2.7×10^{-1}	2.2×10^{-1}	9.5×10^{-2}
H_2/CO_2	2.2×10^{-1}	2.8×10^{-1}	2.4×10^{-1}	5.3×10^{-2}
$NH_3 + H_2O/CO_2$	7.4×10^{-2}	8.9×10^{-2}	9.3×10^{-2}	5.3×10^{-2}
$H_2 : H_2O : CO_2 = 1 : 0.5 : 1$	N/A	3.4×10^{-1}	N/A	N/A
$H_2 : H_2O : CO_2 = 0.5 : 1 : 1$	N/A	6.7×10^{-1}	N/A	N/A
$H_2 : H_2O : CO_2 = 0.5 : 0.5 : 1$	N/A	4.0×10^{-1}	N/A	N/A
$H_2 : H_2O : CO_2 = 1 : 1 : 1$	N/A	6.0×10^{-1}	N/A	N/A
$H_2 : H_2O : CO_2 = 2 : 2 : 1$	N/A	4.5×10^{-1}	N/A	N/A
Without UV				
H_2O/CO_2	1.3×10^{-3}	3.6×10^{-3}	4.7×10^{-3}	2.7×10^{-3}
H_2/CO_2	1.7×10^{-3}	3.1×10^{-3}	4.3×10^{-3}	2.9×10^{-3}
$NH_3 + H_2O/CO_2$	6.7×10^{-4}	2.9×10^{-3}	3.7×10^{-3}	3.6×10^{-3}

Fe/TiO_2(100) is the highest among the prepared photocatalysts under H_2O/CO_2 and H_2/CO_2 conditions, while that for Fe/TiO_2(500) is the highest among the prepared photocatalysts under $NH_3 + H_2O/CO_2$ condition.

(3) Under the illumination condition without UV light, the molar quantity of CO per weight of photocatalyst for Fe/TiO_2(500) is the highest among the prepared photocatalysts irrespective of reductant used, indicating that the larger pulse number is suitable for the illumination condition without UV light.

(4) The CO_2 reduction performance of Fe/TiO_2 under $NH_3 + H_2O/CO_2$ condition is lower compared to that under H_2O/CO_2 and H_2/CO_2 conditions due to complicity of the reaction.

(5) Since a very thick Fe layer covers TiO_2 film for the Fe/TiO_2(1000) and blocks light absorption and reactant contact with TiO_2, the CO_2 reduction performance with Fe/TiO_2(1000) is very poor.

(6) In this study, the highest CO_2 reduction performance of Fe/TiO_2, that is, the molar quantity of CO per weight of photocatalyst for Fe/TiO_2(100), is obtained under $H_2 + H_2O/CO_2$ condition, and the best moral ratio of total reductants to CO_2 is found to be 1.5 : 1.

Conflicts of Interest

The authors declare that there is no conflict of interest regarding the publication of this paper.

Acknowledgments

The authors would like to gratefully thank JSPS KAKENHI (Grant no. 16K06970) and joint research program of the

Institute of Materials and Systems for Sustainability, Nagoya University, for the financial support of this work.

References

[1] World Data Center for Greenhouse Gases, http://ds.data.jma.go.jp/gmd/wdcgg/wdcgg.html.

[2] S. Das and W. M. A. W. Daud, "Photocatalytic CO_2 transformation into fuel: a review on advances in photocatalyst and photoreactor," *Renewable and Sustainable Energy Reviews*, vol. 39, pp. 765–805, 2014.

[3] T. Sakakura, J. C. Choi, and H. Yasuda, "Transformation of carbon dioxide," *Chemical Reviews*, vol. 107, no. 6, pp. 2365–2387, 2007.

[4] K. Adachi, K. Ohta, and T. Mizuno, "Photocatalytic reduction of carbon dioxide to hydrocarbon using copper-loaded titanium dioxide," *Solar Energy*, vol. 53, no. 2, pp. 187–190, 1994.

[5] A. Cybula, M. Klein, A. Z. Jurek, M. Janczarek, and A. Zaleska, "Carbon dioxide photoconversion. The effect of titanium dioxide immobilization conditions and photocatalyst type," *Physicochemical Problems of Mineral Processing*, vol. 48, no. 1, pp. 159–167, 2012.

[6] G. R. Dey, A. D. Belapurkar, and K. Kishore, "Photo-catalytic reduction of carbon dioxide to methane using TiO_2 as suspension in water," *Journal of Photochemistry and Photobiology A*, vol. 163, no. 3, pp. 503–508, 2004.

[7] P. N. Paulino, V. M. M. Salim, and N. S. Resende, "Zn-Cu promoted TiO_2 photocatalyst for CO_2 reduction with H_2O under UV light," *Applied Catalysis B: Environmental*, vol. 185, pp. 362–370, 2016.

[8] L. Liu, C. Zhao, J. T. Miller, and Y. Li, "Mechanistic study of CO_2 photoreduction with H_2O on Cu/TiO_2 nanocomposites by in situ x-ray absorption and infrared spectroscopies," *The Journal of Physical Chemistry C*, vol. 121, pp. 490–499, 2017.

[9] S. Kaneco, H. Kurimoto, Y. Shimizu, K. Ohta, and T. Mizuno, "Photocatalytic reduction of CO_2 using TiO_2 powders in supercritical fluid CO_2," *Energy*, vol. 24, no. 1, pp. 21–30, 1999.

[10] M. M. Gui, S. P. Chai, B. Q. Xu, and A. R. Mohamed, "Enhanced visible light responsive MWCNT/TiO_2 core-shell nanocomposites as the potential photocatalyst for reduction of CO_2 into methane," *Solar Energy Materials & Solar Cells*, vol. 122, pp. 183–189, 2014.

[11] L. L. Tan, W. J. Ong, S. P. Chai, and A. R. Mohamed, "Noble metal modified reduced graphene oxide/TiO_2 ternary nanostructures for efficient visible-light-driven photoreduction of carbon dioxide into methane," *Applied Catalysis B: Environmental*, vol. 166-167, pp. 251–259, 2015.

[12] A. A. Beigi, S. Fatemi, and Z. Salehi, "Synthesis of nanocomposite CdS/TiO_2 and investigation of its photocatalytic activity of CO_2 reduction to CO and CH_4 under visible light irradiation," *Journal of CO_2 Utilization*, vol. 7, pp. 23–29, 2014.

[13] B. Michalkiewicz, J. Majewska, G. Kadziolka, K. Bubacz, S. Mozia, and A. W. Morawski, "Reduction of CO_2 by adsorption and reaction on surface of TiO_2-nitorogen modified photocatalyst," *Journal of CO_2 Utilization*, vol. 5, pp. 47–52, 2014.

[14] C. W. Lee, R. A. Kourounioti, J. C. S. Wu et al., "Photocatalytic conversion of CO_2 to hydrocarbons by light-harvesting complex assisted Rh-doped TiO_2 photocatalyst," *Journal of CO_2 Utilization*, vol. 5, pp. 33–40, 2014.

[15] O. Ozcan, F. Fukruk, E. U. Akkaya, and D. Uner, "Dye sensitized CO_2 reduction over pure and platinized TiO_2," *Topics in Catalysis*, vol. 44, no. 4, pp. 523–528, 2007.

[16] J. A. Wang, R. L. Ballesteros, T. Lopez et al., "Quantitative determination of titanium lattice defects and solid-state reaction mechanism in iron-doped TiO_2 photocatalysts," *The Journal of Physical Chemistry B*, vol. 105, pp. 9692–9698, 2001.

[17] L. Laokiat, P. Khemthong, N. Grisdanurak, P. Sreearunothai, W. Pattanasiriwisawa, and W. Klysubun, "Photocatalytic degradation of benzene, toluene, ethylbenzene, and xylene (BTEX) using transition metal-doped titanium dioxide immobilized on fiberglass cloth," *Korean Journal of Chemical Engineering*, vol. 29, no. 3, pp. 377–383, 2012.

[18] Z. Ambrus, N. Balazs, T. Alapi et al., "Synthesis, structure and photocatalytic properties of Fe(III)-doped TiO_2 prepared from $TiCl_3$," *Applied Catalysis B: Environmental*, vol. 81, no. 1-2, pp. 27–37, 2008.

[19] K. Nagaveni, M. S. Hegde, and G. Madras, "Structure and photocatalytic activity of $Ti_{1-x}M_xO_{2\pm\delta}$ (M = W, V, Ce, Zr, Fe, and Cu) synthesized by solution combustion method," *The Journal of Physical Chemistry B*, vol. 108, pp. 20204–20212, 2004.

[20] S. Das and W. M. A. W. Daud, "Photocatalytic CO_2 transformation into fuel: a review on advances in photocatalyst and photoreactor," *Renewable and Sustaibnable Energy Reviews*, vol. 39, pp. 765–805, 2014.

[21] H. Sun and S. Wang, "Research advances in the synthesis of nanocarbon-based photocatalysts and their applications for photocatalytic conversion of carbon dioxide to hydrocarbon fuels," *Energy & Fuels*, vol. 28, pp. 22–36, 2014.

[22] L. Liu and Y. Li, "Understanding the reaction mechanism of photocatalytic reduction of CO_2 with H_2O on TiO_2-based photocatalysts: a review," *Aerosol and Air Quality Research*, vol. 14, pp. 453–469, 2014.

[23] Y. Sohn, W. Huang, and F. Taghipour, "Recent progress and perspectives in the photocatalytic CO_2 reduction of Ti-oxide-based nanomaterials," *Applied Surface Science*, vol. 396, pp. 1696–1711, 2017.

[24] Z. Goren, I. Willner, A. J. Nelson, and A. J. Frank, "Selective photoreduction of CO_2/HCO_3^- to formate by aqueous suspensions and colloids of Pd-TiO_2," *Journal of Physical Chemistry*, vol. 94, no. 9, pp. 3784–3790, 1990.

[25] I. H. Tseng, W. C. Chang, and J. C. S. Wu, "Photoreduction of CO_2 using sol-gel derived titania and titania-supported copper catalysts," *Applied Catalysis B*, vol. 37, no. 1, pp. 37-38, 2002.

[26] A. Nishimura, N. Sugiura, M. Fujita, S. Kato, and S. Kato, "Influence of preparation conditions of coated TiO_2 film on CO_2 reforming performance," *Kagaku Kogaku Ronbunshu*, vol. 33, no. 2, pp. 146–153, 2007.

[27] Y. Kohno, H. Hayashi, S. Takenaka, T. Tanaka, T. Funabiki, and S. Yoshida, "Photo-enhanced reduction of carbon dioxide with hydrogen over Rh/TiO_2," *Journal of Photochemistry and Photobiology a*, vol. 126, no. 1–3, pp. 117–123, 1999.

[28] K. R. Thampi, J. Kiwi, and M. Gratzel, "Methanation and photo-methanation of carbon dioxide at room temperature and atmospheric pressure," *Nature*, vol. 327, pp. 506-507, 1987.

[29] T. Abe, M. Tanizawa, K. Watanabe, and A. Taguchi, "CO_2 methanation property of Ru nanoparticle-loaded TiO_2

prepared by a polygonal barrel-sputtering method," *Energy & Environmental Science*, vol. 2, pp. 315–321, 2009.

[30] C. C. Lo, C. H. Hung, C. S. Yuan, and J. F. Wu, "Photoreduction of carbon dioxide with H_2 and H_2O over TiO_2 and ZrO_2 in a circulated photocatalytic reactor," *Solar Energy Materials & Solar Cells*, vol. 91, no. 19, pp. 1765–1774, 2007.

[31] G. Mahmodi, S. Sharifnia, M. Madani, and V. Vatanpour, "Photoreduction of carbon dioxide in the presence of H_2, H_2O and CH_4 over TiO_2 and ZrO photocatalysts," *Solar Energy*, vol. 97, pp. 186–194, 2013.

[32] Y. Kohno, T. Tanaka, T. Funabiki, and S. Yoshida, "Photoreduction of CO_2 with H_2 over ZrO_2. A study on interaction of hydrogen with photoexcited CO_2," *Physical Chemistry Chemical Physics*, vol. 2, pp. 2635–2639, 2000.

[33] K. Teramura, H. Tsuneoka, T. Shishido, and T. Tanaka, "Effect of H_2 gas as a reductant on photoreduction of CO_2 over a Ga_2O_3 photocatalyst," *Chemical Physics Letters*, vol. 467, no. 1–3, pp. 191–194, 2008.

[34] Y. Kohno, T. Tanaka, T. Funabiki, and S. Yoshida, "Identification and reactivity of a surface intermediate in the photoreduction of CO_2 with H_2 over ZrO_2," *Journal of the Chemical Society, Faraday Transactions*, vol. 94, no. 13, pp. 1875–1880, 1998.

[35] K. Teramura, T. Tanaka, H. Ishikawa, Y. Kohno, and T. Funabiki, "Photocatalytic reduction of CO_2 to CO in the presence of H_2 or CH_4 as a reductant over MgO," *The Journal of Physical Chemistry B*, vol. 108, pp. 346–354, 2004.

[36] Y. Izumi, "Recent advances in the photocatalytic conversion of carbon dioxide to fuels with water and/or hydrogen using solar energy and beyond," *Coordination Chemistry Reviews*, vol. 257, pp. 171–186, 2013.

[37] J. Nemoto, N. Goken, H. Ueno, and M. Kaneko, "Photodecomposition of ammonia to dinitrogen and dihydrogen on platinized TiO_2 nanoparticles in an aqueous solution," *Journal of Photochemistry and Photobiology A: Chemistry*, vol. 185, no. 2-3, pp. 295–300, 2007.

[38] A. Nishimura, X. Zhao, T. Hayakawa, N. Ishida, M. Hirota, and E. Hu, "Impact of overlapping Fe/TiO_2 prepared by sol-gel and dip-coating process on CO_2 reduction," *International Journal of Photoenergy*, vol. 2016, Article ID 2392581, 12 pages, 2016.

[39] Japan Society of Mechanical Engineering, *Heat Transfer Hand Book*, Maruzen, Tokyo, 1st edition, 1993.

[40] C. Zhao, L. Liu, G. Rao et al., "Synthesis of novel MgAl layered double oxide grafted TiO_2 cuboids and their photocatalytic activity on CO_2 reduction with water vapor," *Catalysis Science & Technology*, vol. 5, pp. 3288–3295, 2015.

[41] Y. Wang, F. Wang, Y. Chen et al., "Enhanced photocatalytic performance of ordered mesoporous Fe-doped CeO_2 catalysts for the reduction of CO_2 with H_2O under simulated solar irradiation," *Applied Catalysis B: Environmental*, vol. 147, pp. 602–609, 2014.

[42] J. Jensen, M. Mikkelsen, and F. C. Krebs, "Flexible substrates as basis for photocatalytic reduction of carbon dioxide," *Solar Energy Materials & Solar Cells*, vol. 95, no. 11, pp. 2949–2958, 2011.

[43] G. Marci, E. L. G. Lopez, and L. Palmisano, "Photocatalytic CO_2 reduction in gas-solid regime in the presence of H_2O by using GaP/TiO_2 composite as photocatalyst under simulated solar light," *Catalysis Communications*, vol. 53, pp. 38–41, 2014.

[44] G. Song, F. Xin, J. Chen, and X. Yin, "Photocatalytic reduction of CO_2 in cyclohexanol on CdS-TiO_2 heterostructured photocatalyst," *Applied Catalysis A: General*, vol. 473, pp. 90–95, 2014.

[45] G. Song, F. Xin, and X. Yin, "Photocatalytic reduction of carbon dioxide over $ZnFe_2O_4$/TiO_2 nanobelts heterostructure in cyclohexanol," *Journal of Colloid and Interface Science*, vol. 442, pp. 60–66, 2015.